



Optical properties of dissolved organic matter in throughfall and stemflow vary across tree species and season in a temperate headwater forest

Kevin A. Ryan · Thomas Adler · Ann T. Chalmers · Julia Perdrial ·
Stephen Sebestyen · James B. Shanley · Aron Stubbins

Received: 29 April 2022 / Accepted: 6 October 2022

This is a U.S. Government work and not under copyright protection in the US; foreign copyright protection may apply 2022

Abstract Tree-derived dissolved organic matter (DOM) comprises a significant carbon flux within forested watersheds. Few studies have assessed the optical properties of tree-derived DOM. To increase understanding of the factors controlling tree-derived DOM quality, we measured DOM optical properties, dissolved organic carbon (DOC) and calcium concentrations in throughfall and stemflow for 17 individual rain events during summer and fall in a temperate deciduous forest in Vermont, United States. DOC and calcium fluxes in throughfall and stemflow were enriched on average 4 to 70 times incident fluxes in rain. A multiway model was developed using absorbance and fluorescence spectroscopy to further characterize DOM optical properties. Throughfall

contained a higher percentage of protein-like DOM fluorescence than stemflow while stemflow was characterized by a higher percentage of humic-like DOM fluorescence. DOM absorbance spectral slopes in yellow birch (*Betula alleghaniensis*) stemflow were significantly higher than in sugar maple (*Acer saccharum*) stemflow. DOM optical metrics were not influenced by rainfall volume, but percent protein-like fluorescence increased in throughfall during autumn when leaves senesced. Given the potential influence of tree-derived DOM fluxes on receiving soils and downstream ecosystems, future modeling of DOM transport and soil biogeochemistry should represent the influence of differing DOM quality in throughfall and stemflow across tree species and seasons.

Responsible Editor: Penny Johnes.

Supplementary Information The online version contains supplementary material available at <https://doi.org/10.1007/s10533-022-00985-x>.

K. A. Ryan
Department of Marine and Environmental Sciences,
Northeastern University, Boston, MA, USA

K. A. Ryan (✉)
U.S. Geological Survey, New York Water Science Center,
425 Jordan Rd, Troy, NY 12180, USA
e-mail: kryan@usgs.gov

T. Adler · J. Perdrial
Department of Geology, University of Vermont,
Burlington, VT, USA

Keywords Dissolved organic matter · Throughfall · Stemflow · Forested watersheds · Carbon cycling · Fluorescence spectroscopy

A. T. Chalmers · J. B. Shanley
U.S. Geological Survey, Montpelier, VT, USA

S. Sebestyen
U.S. Forest Service Northern Research Station,
Grand Rapids, MN 55744, USA

A. Stubbins
Departments of Chemistry and Chemical Biology
and Civil and Environmental Engineering, Northeastern
University, Boston, MA, USA

Introduction

Terrestrial vegetation exerts substantial influence on global hydrological and biogeochemical cycles (Hutjes et al. 1998). In forested ecosystems, the first interactions between water inputs and terrestrial carbon sources typically occur within the tree canopy, where precipitation is partitioned into throughfall and stemflow. Throughfall is precipitation that falls on and through the canopy to the forest floor and typically comprises the largest fraction of incident precipitation (Hewlett 1982; Levia and Frost 2006). Stemflow is precipitation that moves along tree surfaces to the base of tree trunks and accounts for a lower percentage of total intercepted rainfall (< 10%) in forests globally (Levia and Germer 2015). Quantifying the influence of vegetation on aquatic solute dynamics in forested ecosystems is of particular importance because tree canopies globally are the primary interceptor of continental rainfall (Angelini et al. 2011).

Throughfall and stemflow are enriched in dissolved organic matter (DOM) and other solutes relative to precipitation (Ponette-González et al. 2020; Van Stan and Stubbins 2018). Meteorological conditions such as the size of precipitation events influence solute fluxes in throughfall and stemflow where solutes are generally diluted by increasing water input (Siegert et al. 2017). However, climate change is altering the hydroclimatic factors influencing fluxes of these biogeochemically active solutes. In the eastern United States, intensification of the water cycle is increasing rain event frequency and intensity (Huntington et al. 2009), potentially accelerating the transfer of tree-derived carbon and nutrients in throughfall and stemflow to forest soils. Dissolved organic carbon (DOC) in throughfall and stemflow can be highly biolabile with 10 to 70% DOC being respired in laboratory incubations over several days (Behnke et al. 2022; Howard et al. 2018; Qualls and Haines 1992). The periodic supply of water and biolabile carbon in throughfall and stemflow induce ecological hot moments that feed downstream microbial communities (McClain et al. 2003; Qualls 2020). Storm-driven fluxes of tree-derived DOM are delivered more frequently through time to the forest floor than annual leaf fall, which occurs predominantly as a pulse in fall. At both annual and event scales, tree-derived DOM fluxes can also be several times larger than fluvial export from forests (McDowell and Likens

1988; Ryan et al. 2021a). Thus, forested ecosystems internally produce and process large quantities of biogeochemically active DOM. The influence of these tree-derived DOM fluxes on downstream ecosystems remains poorly understood (Van Stan and Stubbins 2018). Tracing tree-derived DOM is necessary for accurately accounting for terrestrial-to-aquatic ecosystem carbon transfers which represent a significant flux within the global carbon cycle (Drake et al. 2018).

The downstream fate of DOM washed and leached from forest vegetation is influenced by DOM chemical composition. Previous studies have used molecular spectroscopy and mass spectrometry to show tree-derived DOM is a complex mixture of aliphatic and aromatic molecules with fluorophores resembling both protein-like and humic-like fluorescence derived from lignin-degradation byproducts, freshly produced biomolecules, and atmospheric deposition (Hernes et al. 2017; Inamdar et al. 2012; Levia et al. 2012; Stubbins et al. 2017; Van Stan et al. 2017). These studies agree with more abundant studies of leaf litter and bark chemistry characterized as biolabile polyphenols (Cuss and Guéguen 2015; Tanase et al. 2019). While absorbance and fluorescence features of DOM have been widely used to characterize DOM in freshwaters (Fellman et al. 2010), reports of DOM optical properties in throughfall and stemflow are rare in comparison to reports of DOC concentrations (Inamdar et al. 2011; Singh et al. 2015; Van Stan et al. 2017). Whereas forest type and climate are known to influence quantities of DOC and other solutes in throughfall and stemflow (Henderson et al. 1977; Ponette-González et al. 2016), less well known are the factors influencing DOM quality. Factors known to influence throughfall and stemflow water fluxes such as precipitation amount, intensity, wind direction, tree species and tree morphology may also influence tree-derived DOM quality. DOM optical properties have been shown to differ among tree species in leaf litter leachate (Cuss and Gueguen 2013; Wheeler et al. 2017) and in throughfall and stemflow from different tree species (Levia et al. 2012; Stubbins et al. 2017; Van Stan et al. 2017). Seasonal variations in throughfall solute dynamics have been documented particularly for temperate deciduous forests with distinct phenological seasons (or “phenoseasons”) (Van Stan et al. 2012). However, more data are needed to quantify changes in tree-derived DOM quality due to

phenoseason to inform ecosystem models. Characterizing and tracing the optical properties of tree-derived DOM is also of particular concern to humans because tree-derived DOM is a known precursor to harmful disinfection byproducts generated during drinking water treatment (Chen et al. 2019; Chow et al. 2009). Thus, optical techniques can be important monitoring tools for assessing the quantity and timing of disinfection byproduct precursors exported from forested watersheds.

Given that tree-derived DOM fluxes can be several times greater than stream fluxes draining the same forest (Ryan et al. 2021a), subtle changes in DOM quality could have important implications for catchment carbon cycling. Thus, further work is warranted to describe how tree-derived DOM quality varies among precipitation, throughfall, and stemflow. Our objective in this study was to advance understanding of the variability of tree-derived DOM optical properties among flow paths, tree species, event size and season. We present concentrations and optical properties of DOM in throughfall and stemflow in a temperate forested watershed in Vermont, USA. We hypothesized that DOM optical properties will differ between throughfall and stemflow and with species and season. We include calcium in this study because it is an essential macronutrient for plant growth and a dominant inorganic ion by mass in natural waters that provides context for inorganic solute dynamics to compare with DOM dynamics. These results add to the limited literature reporting spatial and seasonal dynamics of tree-derived DOM quality and provide foundational information applicable to quantifying DOM sources and carbon cycling in ecosystem models.

Methods

Site description

The study area was the 40.5-ha headwater forested W-9 catchment in the Sleepers River Research Watershed in Vermont, USA (elevation range 519 to 672 m; Fig. 1). Mean annual air temperature for the site is 4.8 °C from 1991 to 2018, and snowfall comprises 20%–30% of annual precipitation primarily between November and April (Shanley 2000; Shanley et al. 2021). Trees in the watershed have not been

selectively harvested since 1960 when it came under management of United States governmental research agencies (Shanley et al. 2015). Dominant tree species are sugar maple (*Acer saccharum* Marsh.), yellow birch (*Betula alleghaniensis* Britt), and white ash (*Fraxinus americana* Ehrh.), with minor amounts of balsam fir (*Abies balsamea* L.), red spruce (*Picea rubens* Sarg.), and American beech (*Fagus grandifolia* Ehrh.). A survey completed in 2011 of 404 living trees measured in 76 plots (100 m² each) across the watershed found that sugar maple and yellow birch comprised 75% and 11% of the total basal area, respectively (white ash=8%). Mean diameter at breast height (DBH) for sugar maple and yellow birch was 26.4 cm ($n=296$) and 29.2 cm ($n=37$), respectively (white ash=35.7 cm; $n=19$). The forest has no substantial tree stress or mortality from legacy acid deposition in the area due to well-buffered soils (Shanley et al. 2004).

Sample collection and processing

Throughfall and stemflow were collected in W-9 for 17 rain events from June to November 2018. Throughfall was collected along four transects of 3.0 m each and one transect of 12.2 m using aluminum troughs secured 80 cm above the forest floor and draining downslope to plastic collection bins. Coarse plastic mesh covered the troughs to exclude leaves and other debris. Stemflow was collected from sugar maple (*Acer saccharum* Marsh.) and yellow birch (*Betula alleghaniensis* Britt) trees which together comprise the dominant hardwood species in the watershed (Park et al. 2008). Stemflow was collected from two mature trees of each species using low-density polyethylene plastic collars sealed to the bark with silicone caulk. The stemflow tubing drained to a sealed plastic bucket. The depth of standing water in throughfall and stemflow collectors was measured after each rain event and converted to volume using a depth to volume calibration curve established for each collector type. Stemflow tree diameter at breast height ranged from 30 to 33 cm and canopy area ranged from 52 to 107 m² (Table S1). Throughfall and stemflow collectors were cleaned with a brush and deionized water prior to and after all measured precipitation events. All sampling materials were precleaned with acidified deionized water (pH 2), triple rinsed with deionized water, and rinsed with sample water

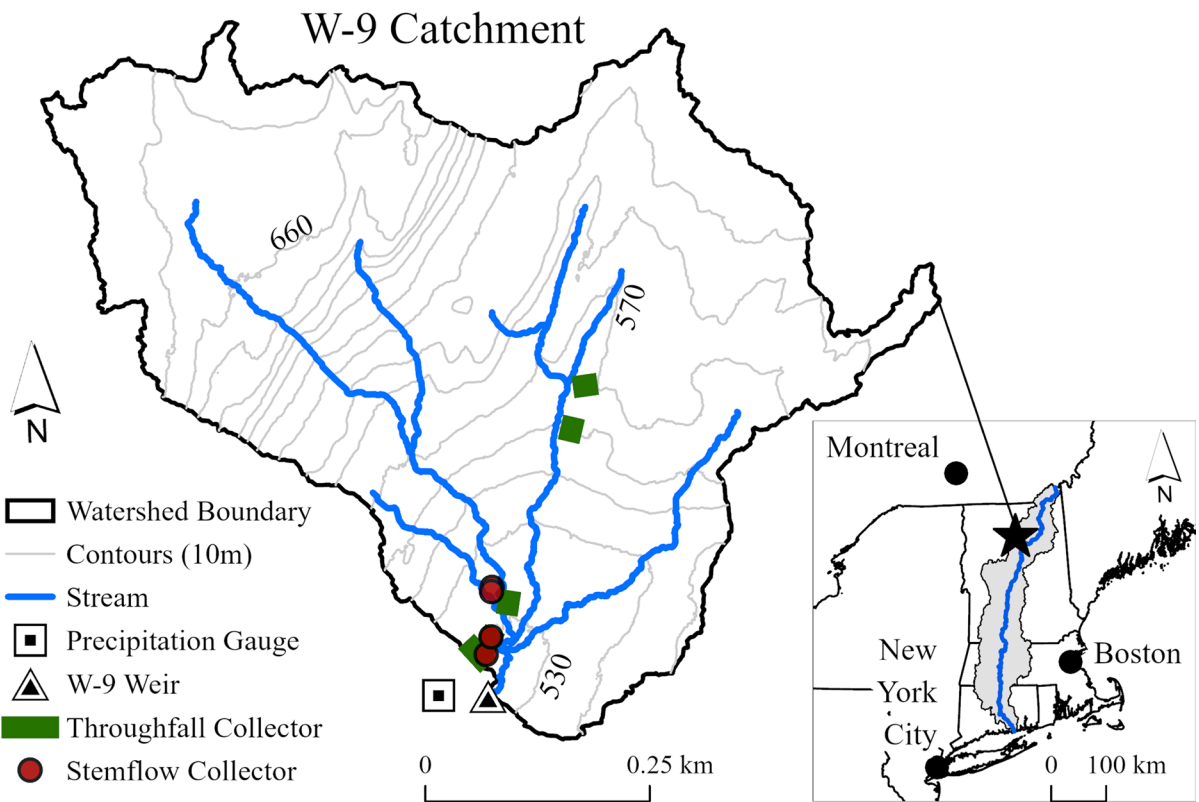


Fig. 1 Map of precipitation, throughfall and stemflow collection locations (Catchment outlet: $44^{\circ} 29' 26''$ N, $72^{\circ} 09' 44''$ W NAD27)

prior to collection. Bulk precipitation, throughfall and stemflow samples were filtered on site using $0.22\text{ }\mu\text{m}$ filters (polyethersulphone, Waterra) after each rain event. Precipitation samples in this study refer only to rainfall as no snow or ice events were measured during the study period.

Solute concentrations

Aliquots of each sample for analysis of DOC were transferred to pre-combusted glass vials and acidified to pH 2 with 6 N hydrochloric acid (HCl) and refrigerated (6°C) in the dark until analysis within 4 weeks of sampling. DOC was measured as non-purgeable organic carbon using a high-temperature catalytic combustion instrument (detection limit: 0.024 mg-C L^{-1} ; TOC-L by Shimadzu). Calibration standards were prepared using a potassium hydrogen phthalate stock solution in MilliQ water (1000 mg-C L^{-1}). Dissolved calcium (Ca^{2+}) was measured at the Forestry Sciences Laboratory of the Northern Research Station

(USDA Forest Service) according to Sebestyen et al. (2020) using inductively coupled plasma optical emission spectroscopy (ICP-OES; detection limit: $0.05\text{ mg-Ca}^{2+}\text{ L}^{-1}$). Additional nutrients and major ions including iron were measured but were excluded from further analysis due to values lower than the analytical limits of detection (15 to 85% of samples). All solute data are available in the accompanying data release (Ryan et al. 2021b).

Optical measurements

Absorbance and fluorescence of DOM were measured on filtered, non-acidified sample aliquots using an Aqualog™ Fluorescence and Absorbance Spectrometer and 1-cm quartz cuvettes (Horiba, Irvine, CA, USA). Samples were stored at 6°C in the dark and equilibrated to room temperature (21 to 23°C) immediately prior to analysis within 2 weeks of sampling. Absorbance spectra of chromophoric DOM (CDOM) were measured from 200 to 600 nm

and blank corrected using ultrapure water (Milli-Q, Millipore). Excitation-Emission-Matrices (EEMs) were generated by recording fluorescence emission from 212 to 619 nm (1 nm intervals) during excitation from 242 to 596 nm (5 nm intervals). Samples with raw absorbance values exceeding 2 absorbance units were diluted to below 0.3 absorbance units to ensure greater than 50% transmission for all samples (Hansen et al. 2018). Lamp and cuvette performance were monitored daily throughout data collection. Fluorescence EEMs of ultrapure Milli-Q water (Millipore) blanks were collected daily.

Data analysis

Rain event water yields of throughfall and stemflow were calculated by normalizing the volume of water collected to the surface area of the trough or the canopy area, respectively. Throughfall and stemflow event solute yields were calculated by multiplying the event water yield by the concentrations in the bulk event water sample. To assess stemflow water yield efficiency and solute enrichment to the basal area for each tree with respect to precipitation and throughfall, dimensionless funneling ratios (FR) and flux-based enrichment ratios (ER) were calculated for each tree and stemflow event (Levia and Germer 2015) (Eq. 1, 2),

$$FR = \frac{S_Y}{P \times B} \quad (1)$$

$$ER_{S,P} = \frac{S_Y \times C_S}{P \times B \times C_P} \quad (2)$$

where S_Y is the stemflow event water yield (mm^3), P is the precipitation event depth (mm), B is the tree basal area (mm^2), and C_S and C_P are the solute concentrations of stemflow and precipitation, respectively. The flux-based enrichment ratios in throughfall compared to precipitation were also calculated (Eq. 3),

$$ER_{T,P} = \frac{T \times C_T}{P \times C_P} \quad (3)$$

where T is the throughfall event yield (mm), and C_T is the solute concentration in throughfall.

Napierian absorption coefficients were calculated according to Eq. 4:

$$a = 2.303 \times \frac{A}{l} \quad (4)$$

where A is absorbance and l is the path length in meters (Kirk 1994). Specific UV absorbance at 254 nm (SUVA_{254} , $\text{L mg-C}^{-1} \text{m}^{-1}$), was calculated by dividing the decadic absorption coefficient at 254 nm (m^{-1}) by the DOC concentration (mg-C L^{-1}) for each sample (Weishaar et al. 2003). Higher SUVA_{254} values indicate higher absorbance per unit carbon due generally to increased aromaticity of the DOM (Weishaar et al. 2003). The slopes of log-linearized absorbance spectra between 275 and 295 nm ($S_{275:295}$) were calculated according to (Helms et al. 2008). Decreasing $S_{275:295}$ has been associated with increasing molecular weight in estuary waters (Helms et al. 2008).

Fluorescence EEMs were blank subtracted and corrected for instrument-specific bias and inner filter effects following Murphy et al. (2013). Each preprocessed EEM was normalized to the Raman peak area of the blank collected daily (Lawaetz and Stedmon 2009). Rayleigh and Raman scatter interferences were removed and were not interpolated prior to further data analysis. To characterize the fluorescent DOM quality of throughfall and stemflow, we generated a three-dimensional model using parallel factor analysis (PARAFAC). PARAFAC models are useful for identifying uncorrelated fluorophore components contributing to the overall DOM fluorescence within a group of samples (Bro 1997). The PARAFAC model was fit to preprocessed EEMs using the *starDom* R package (Pucher et al. 2019). Precipitation samples were excluded from model development to reduce model noise since these samples had low overall fluorescence. Each EEM was normalized to maximum fluorescence prior to fitting the model to minimize concentration effects on model results. The model was fitted using random initialization (100 starts) under a non-negativity constraint following recommended procedures (Pucher et al. 2019). The final PARAFAC model was validated using split-half validation and Tuckers Congruence Coefficients ($\text{TCC} > 0.99$). The sample-specific maximum fluorescence (F_{max}) for each model component was used to compare model results across samples. The final PARAFAC model components were compared to relevant fluorophores reported in the OpenFluor database (Murphy et al. 2014). Conventional fluorescence peaks (B, T, A,

M, C) and indices (FI, freshness, BIX), were also extracted from corrected EEMs using the *staRdom* R package according to the references therein (Coble 1996; Huguet et al. 2009; McKnight et al. 2001; Ohno 2002). All fluorescence indices are reported in the accompanying data release (Ryan et al. 2021b).

As a dominant cation in natural waters, the concentration of Ca^{2+} was used in the interpretation of DOM trends. The molar ratio of Ca^{2+} to DOC was used as a relative indicator of organic versus inorganic solute removal from tree surfaces. All data from individual replicate throughfall and stemflow collectors were used in box plots and summary statistics. However, samples from replicate collectors were averaged prior to assessing relations with event volume or season to reduce the influence of replicate samples on model significance.

The Shapiro–Wilk test and visual inspection of the data using quantile–quantile plots were used to determine when median values or ranges should be reported to reduce the influence of skew on summary statistics. To ascertain the general strength and direction of linear and log-linear solute relations with storm size quantified as rainfall event volume, Pearson's correlation coefficients (r), p-values and coefficients of determination (r^2) were calculated for each solute and flow path. Methods for linear and nonlinear least squares estimation were implemented in R to fit linear and exponential decay models.

Results

Precipitation partitioning

Precipitation, throughfall and stemflow samples were collected for 17 rain events ranging from 3 to 72 mm (median=25 mm). The dataset was skewed toward smaller events with only one event greater than 40 mm and 12 events less than 30 mm (Shapiro–Wilk test $p<0.005$). Throughfall event water yield ranged from 2 to 62 mm (median: 25 mm). Stemflow event water yields ranged from 0.01 to 0.30 mm (median=0.07 mm). Mean (\pm standard deviation) stemflow funneling ratios were greater than one for both sugar maple ($\text{mean}=2.1 \pm 1.5$) and yellow birch (3.0 ± 1.8) indicating stemflow input to the forest floor at a tree base generally exceeded mean

areal rainfall amounts expected in the absence of the tree.

Dissolved organic carbon and solute concentrations

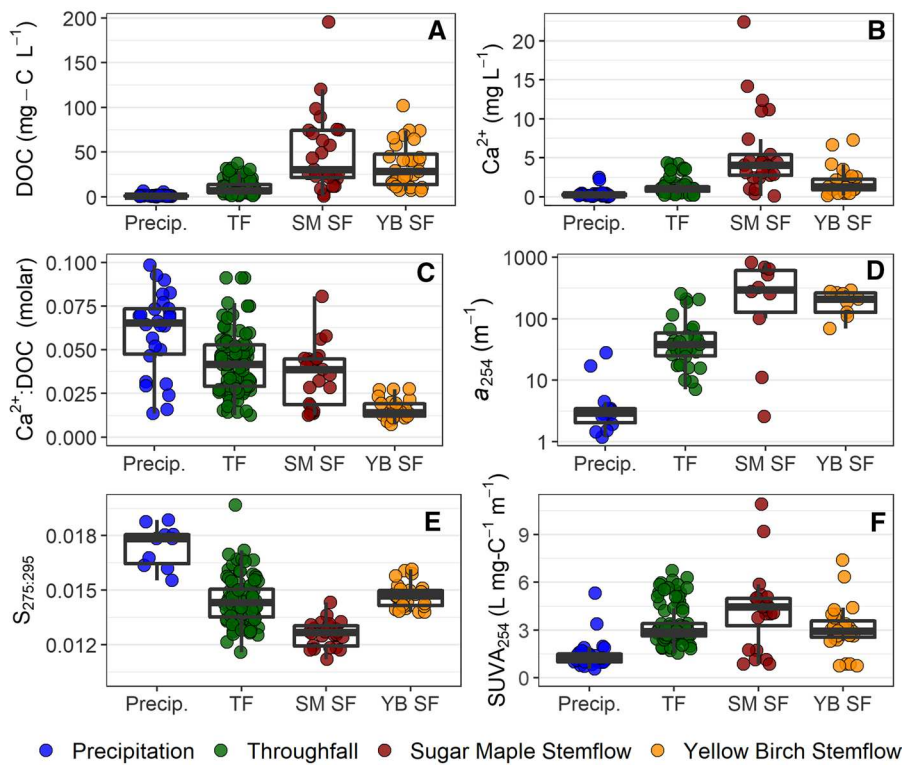
In comparison to precipitation, throughfall and stemflow were enriched in DOC (Fig. 2A). Mean DOC concentrations in mixed stand throughfall ($10 \pm 8.1 \text{ mg-C L}^{-1}$) were lower than for sugar maple ($50 \pm 44 \text{ mg-C L}^{-1}$) and yellow birch ($36 \pm 25 \text{ mg-C L}^{-1}$) stemflow. Median flux-based enrichment ratios for DOC concentrations were higher for sugar maple (76) and yellow birch (72) stemflow than for throughfall (6.3; Table S2). Throughfall and stemflow were also enriched in Ca^{2+} relative to precipitation (Fig. 2B). Calcium concentrations ranged from 0.06 to 2.4 mg L^{-1} in precipitation, 0.2 to 4.4 mg L^{-1} in throughfall, 0.1 to 22 mg L^{-1} in sugar maple stemflow, and 0.2 to 7 mg L^{-1} in yellow birch stemflow (Shapiro Wilk test for normality $p<0.001$). Median flux-based enrichment ratios for Ca^{2+} in throughfall, sugar maple stemflow and yellow birch stemflow were 4, 30, and 15, respectively. The molar ratio of $\text{Ca}^{2+}:\text{DOC}$ ranged from 0.01 to 1.0 and was higher for precipitation than for throughfall or stemflow (Fig. 2C).

Chromophoric dissolved organic matter

Absorbance spectra for throughfall and stemflow decreased roughly exponentially from 250 to 600 nm. Mean Napierian absorbance coefficients at 254 nm (a_{254}) for precipitation ($3.5 \pm 3.0 \text{ m}^{-1}$) were lower than those of throughfall ($68 \pm 48 \text{ m}^{-1}$), sugar maple stemflow ($530 \pm 430 \text{ m}^{-1}$), and yellow birch stemflow ($230 \pm 150 \text{ m}^{-1}$; Fig. 2D). Median enrichment ratios for a_{254} were also higher for sugar maple and yellow birch stemflow (> 200) than for throughfall (24; Table S2).

Spectral slopes between 275 and 295 nm ($S_{275,295}$) for sugar maple stemflow ($\text{mean}=0.014 \pm 0.003 \text{ nm}^{-1}$), yellow birch stemflow ($0.015 \pm 0.001 \text{ nm}^{-1}$) and throughfall ($0.015 \pm 0.001 \text{ nm}^{-1}$) were lower than for precipitation ($0.022 \pm 0.005 \text{ nm}^{-1}$; Fig. 2E). SUVA₂₅₄ values were highest for sugar maple stemflow ($4.4 \pm 2.4 \text{ L mg-C}^{-1} \text{ m}^{-1}$), followed by yellow birch stemflow ($3.1 \pm 1.5 \text{ L mg-C}^{-1} \text{ m}^{-1}$) and throughfall ($3.4 \pm 1.2 \text{ L mg-C}^{-1} \text{ m}^{-1}$).

Fig. 2 Boxplots and jitter plots of **A** dissolved organic carbon (DOC), **B** Ca^{2+} , **C** the molar ratio of Ca^{2+} to DOC, **D** Napierian absorbance coefficient at 254 nm (a_{254}), **E** absorbance spectra slope from 275 to 295 nm ($S_{275:295}$), and **F** specific UV absorbance at 254 nm (SUVA₂₅₄) across flow paths. Boxes depict the median and first and third quartiles. Whiskers extend to the minimum or maximum value no further than 1.5 times the inner quartile range



$\text{mg-C}^{-1} \text{m}^{-1}$), and lowest for precipitation ($1.4 \pm 0.9 \text{ L mg-C}^{-1} \text{m}^{-1}$; Fig. 2F).

Fluorescent dissolved organic matter

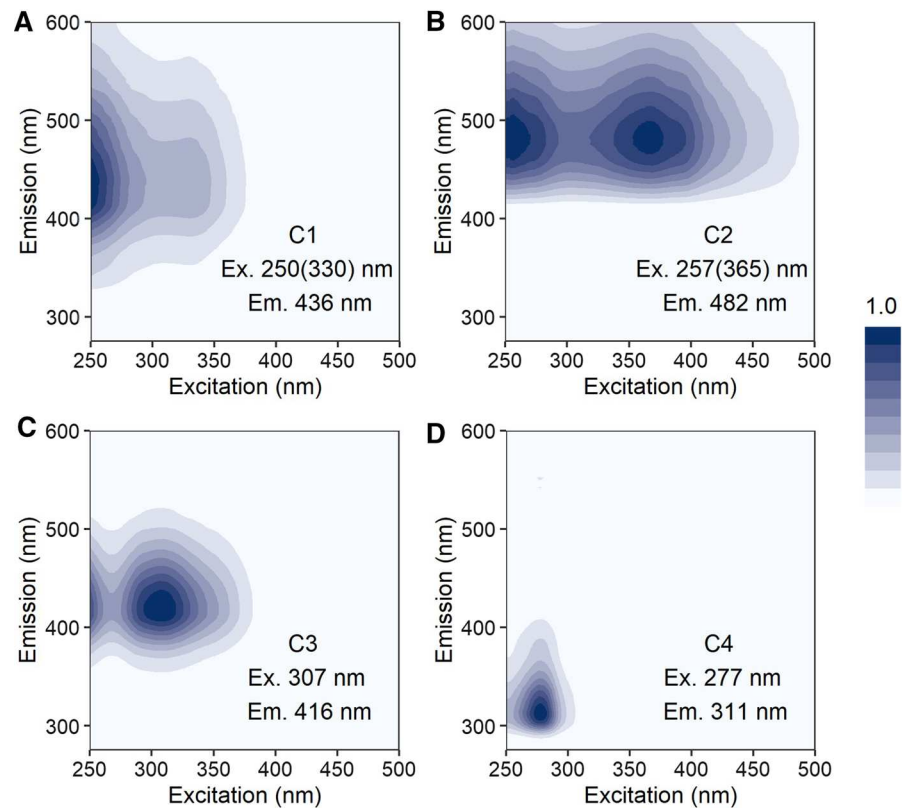
A four-component PARAFAC model (Fig. 3) best described the dataset. PARAFAC model components were classified according to known aquatic DOM fluorescence peaks (Fellman et al. 2010; Hansen et al. 2016). Of the four components, C1, C2, and C3 were classified as representing humic-like DOM fluorescence. C1 and C2 corresponded closely to the classic A and C peaks of humic-like DOM fluorescence. C3 was a blue-shifted humic-like peak similar to peak M (Coble 1996). C4 is similar to classic peak B and is consistent with the optical properties of protein-like or “fresh” DOM, though fluorescence in this region is not necessarily due to free amino acids, proteins, or microbially-derived, freshly produced DOM (Aiken 2014; Coble 1996).

Overall fluorescence intensities (R.U.) followed the order sugar maple stemflow > yellow birch stemflow > throughfall > precipitation (Fig. 4). Peak fluorescence intensities in precipitation EEMs were

10 times lower than for throughfall or stemflow (Fig. 4A). Throughfall was enriched in protein-like fluorescence (C4) compared to stemflow, while sugar maple stemflow was enriched in humic-like fluorescence (C2) compared to throughfall and yellow birch stemflow (Fig. 5A). The ratio of percent humic-like C2 to percent protein-like C4 was found to be useful in discriminating between samples with each flow path clustered separately on a biplot (Fig. 5B; Table S3; ANOVA $p < 0.01$). The percent humic-like components, %C1 and %C3, were not significantly different among all sample types and the percent protein-like component %C4 was not significantly different between sugar maple and yellow birch stemflow (Table S3). Precipitation EEMs were characterized by lower percentages of humic-like (C2) DOM fluorescence and higher overall variability (Fig. 5). The mean fluorescence index was similar for throughfall (1.5) and stemflow (1.4) samples and but higher for precipitation (1.7). The mean biological index was ~ 0.4 for throughfall and stemflow samples but similarly higher for precipitation (0.6).

Median flux-based enrichment ratios for F_{tot} were also higher for sugar maple and yellow birch

Fig. 3 Excitation emission spectra for normalized parallel factor analysis model components. Wavelengths of peak excitation (Ex.) and emission (Em.) for each component are displayed. Secondary excitation peaks are in parentheses



stemflow (> 150) than for throughfall (16; Table S2). Median flux-based enrichment ratios for humic-like fluorescence C2 in throughfall (median > 100) and stemflow (median > 1000) were higher than for DOC concentrations (< 100).

Solute and quality relations with precipitation event size

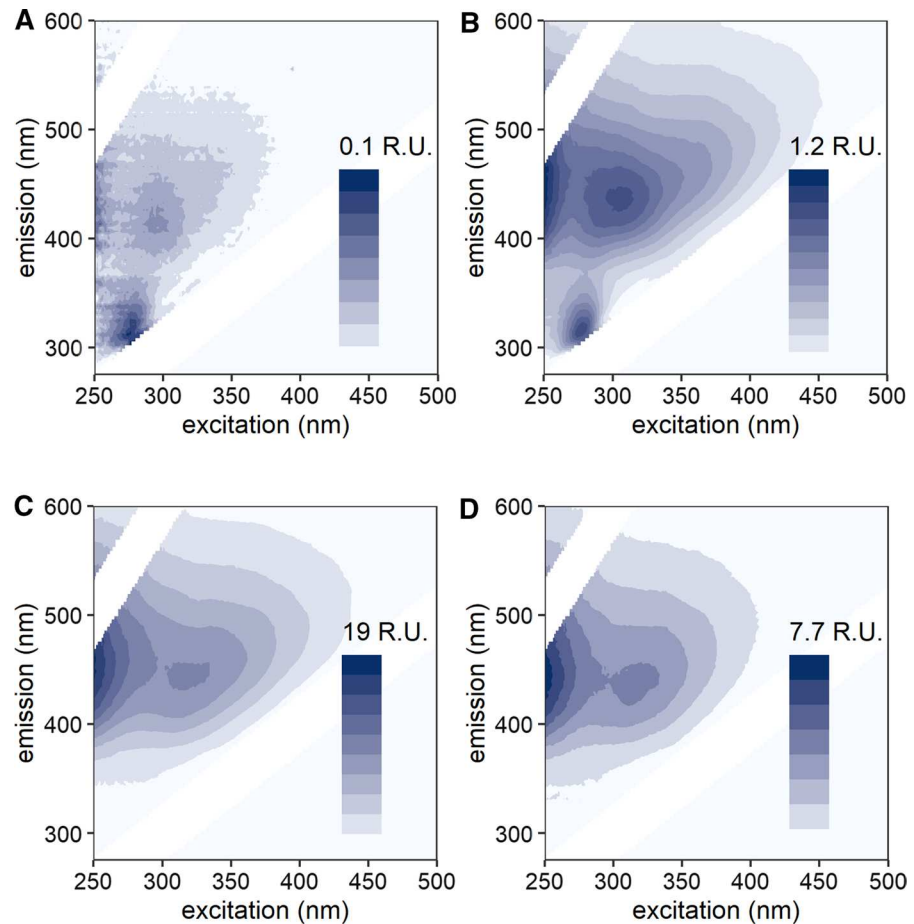
We assessed linear and log-linear relations of concentrations and optical metrics versus precipitation event volume for throughfall and stemflow. Data from replicate collectors were averaged prior to modeling relations with event volume to reduce the influence of replicate samples on model significance. Quantitative variables such as solute concentrations and absorbance and fluorescence intensities displayed significant decreasing trends with increasing event size (Table S4). Since a primary mechanism of decreasing solutes with increasing incident precipitation is dilution, nonlinear models were fit for the selected quantitative parameters DOC, a_{254} , F_{tot} , and Ca^{2+} , showing approximately exponential decreases with

increasing precipitation (Fig. 6). Exponential decay slopes were more similar within sample types for DOC, a_{254} , F_{tot} , and Ca^{2+} than for the same variables across sample types (Fig. 6). For example, the mean (\pm s.d.) of all modeled decay slopes for sugar maple stemflow (0.23 ± 0.06) was higher than for throughfall (0.13 ± 0.04) and yellow birch stemflow (0.08 ± 0.02 ; Table S4). No trends were observed for DOM optical qualitative metrics such as $SUVA_{254}$, absorbance spectral slopes, or percent PARAFAC components.

Seasonal influence on throughfall and stemflow quality

Assessing seasonal influence on throughfall and stemflow concentrations was not possible due to the strong influence of storm event volume on solute flux, the limited number of storms sampled, and an unequal distribution of storms sampled across seasons. However, DOM optical metrics were not significantly influenced by storm event volume ($p > 0.1$; Table S4), allowing assessment of seasonal variability in DOM quality. For instance,

Fig. 4 Example excitation-emission matrices for **A** precipitation, **B** mixed-canopy throughfall, **C** sugar maple stemflow, and **D** yellow birch stemflow. Representative examples were selected based on the median %C2:%C4 ratio within each sample group during September, 2018



SUVA_{254} , percent protein-like fluorescence (%C4), and $\text{Ca}^{2+}:\text{DOC}$ visualized over the sampling period indicate changing throughfall and stemflow quality during the fall season (Fig. 7). SUVA_{254} in throughfall collected in late September and October during leaf senescence ($4.7 \text{ L mg-C}^{-1} \text{ m}^{-1}$; $n=15$) was significantly elevated in comparison to events with mature leaves during summer months (mean = $3.1 \text{ L mg-C}^{-1} \text{ m}^{-1}$; $n=62$; Fig. 7A; t-test p-value < 0.001). Similarly, percent C4 in throughfall collected from fall events (mean = 48%; $n=15$) was higher than in events during summer months (mean = 31%; $n=62$; Fig. 7B; t-test p-value < 0.001). The molar ratio of Ca^{2+} to DOC was also elevated in throughfall during fall storms (0.053 ± 0.023) compared to summer storms (0.041 ± 0.016 ; t-test p-value < 0.1; Fig. 7C). In stemflow, data were more variable across seasons and consistent statistical trends were not found.

Discussion

Precipitation partitioning

The median percentage of precipitation converted to throughfall (96%) was higher than for forests globally (76%; Sadeghi et al. 2020) but more similar to the nearby Hubbard Brook forest (~ 90%) (Leonard 1961). Using the slope of the linear relation of throughfall yield versus event precipitation, Ryan et al. (2021a) estimated that 88% of precipitation is converted to throughfall for the events in this dataset. For both sugar maple and yellow birch, the percentage of precipitation converted to stemflow (median = 0.2%) fell within the lower range of previous studies globally (< 10%; median = 2.2%; Sadeghi et al. 2020). Yellow birch trees (median funneling ratio = 2.5) generated more stemflow per

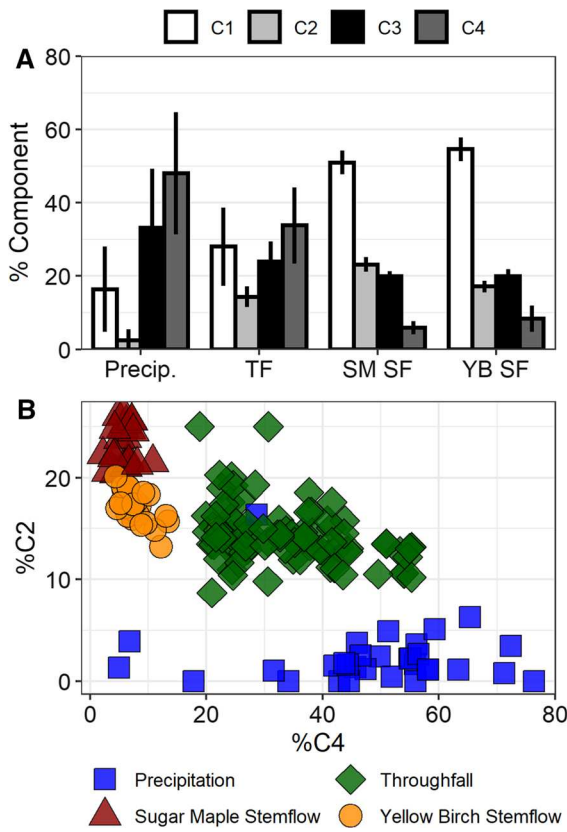


Fig. 5 **A** Mean percent PARAFAC component for each flow path. Error bars represent 1 standard deviation. **B** Percent PARAFAC component C2 (humic-like) versus percent C4 (protein-like) for all samples colored by sample type

canopy area than sugar maple trees (1.7) likely due to differences in bark structure where yellow birch bark is thin and smooth, while sugar maple bark is thick and furrowed (Levia and Herwitz 2005; Levia et al. 2010). Although event size and species were the primary factors assumed to be influencing variability in throughfall and stemflow water yields in this study, unmeasured factors such as wind direction and tree morphology likely impacted results as well (Levia and Frost 2006; Levia and Germer 2015). Overall, precipitation partitioning was typical of temperate deciduous forests thus we expect the event scale solute dynamics discussed below to be applicable to these systems.

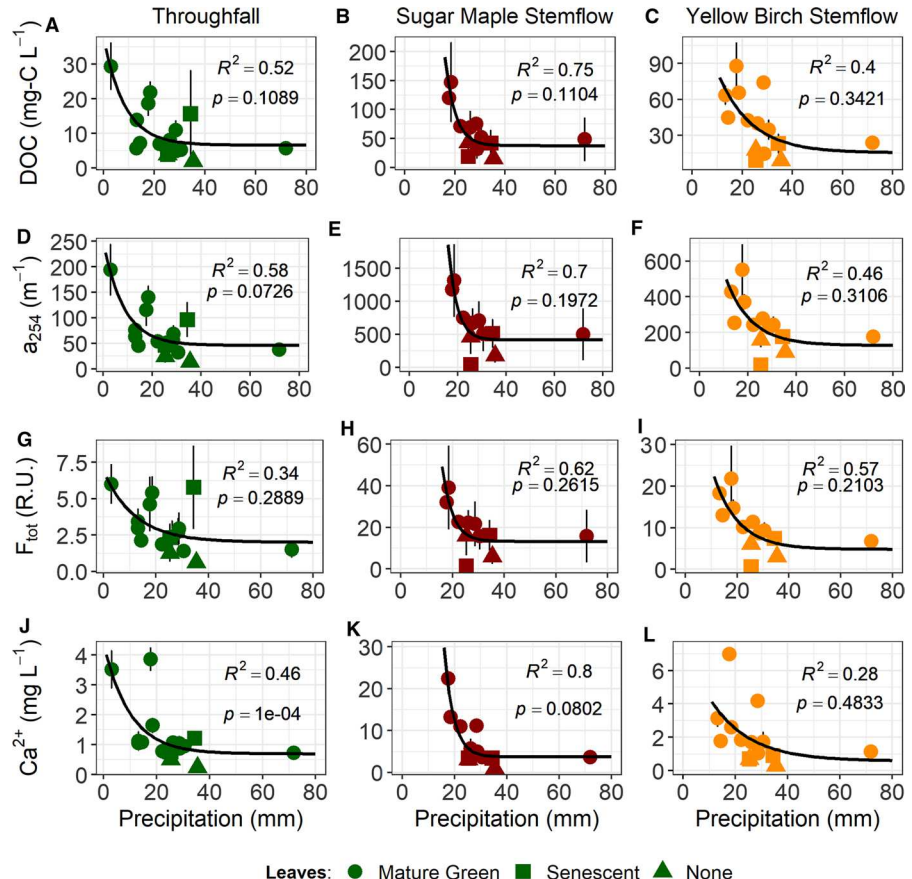
Solute concentrations

DOC concentrations in precipitation (mean = $1.3 \pm 1.2 \text{ mg-C L}^{-1}$) were similar to the long-term average concentration for precipitation at Sleepers River Research Watershed (1.1 mg-C L^{-1}), and fell within the range for rainfall globally (mean = $2.9 \pm 1.9 \text{ mg-C L}^{-1}$; Iavorivska et al. 2016). DOC concentrations in throughfall (mean = $10 \pm 8.1 \text{ mg-C L}^{-1}$) and stemflow (yellow birch = 35 ± 25 ; sugar maple = 50 ± 44) also fell within the ranges previously reported for a variety of forest types (7 to 482 mg-C L^{-1} ; Van Stan and Stubbins 2018). These concentrations are higher than the long-term average stream DOC concentration in W9 (4.1 mg-C L^{-1}) and for rivers globally ($\sim 4 \text{ mg-C L}^{-1}$; Mulholland 2002).

Median Ca^{2+} concentrations in precipitation (0.3 mg L^{-1}) and throughfall (1.0 mg L^{-1}) were similar to those reported for sugar maple and yellow birch throughfall in a nearby broadleaf mixed forest in New Hampshire (precipitation = 0.16 mg L^{-1} ; throughfall = $\sim 1.5 \text{ mg L}^{-1}$; Eaton et al. 1973). Median stemflow concentrations for Ca^{2+} (yellow birch = 1.2 mg L^{-1} ; sugar maple = 4.0 mg L^{-1}) and flux-based enrichment ratios (yellow birch = 15; sugar maple = 29) were also similar to broadleaf stemflow reported in the Mid-Atlantic region (Maryland; 0.8 to 2.7 mg L^{-1} ; ratios = 3 to 15; Levia et al. 2011). Outside of coastal zones, calcium in rainfall is sourced from aeolian erosion, biomass burning, or human activity such as cement production (Ponette-González et al. 2016). The basin is underlain by calcareous rich glacial till (DeKett and Long 1995). Thus, dry deposition of local soil dust and subsequent dissolution may have contributed to calcium fluxes.

The flux-based enrichment ratios of DOC indicated that stemflow (median = ~ 70) was more enriched than throughfall (6), a pattern commonly attributed to the increased contact time with tree surfaces per unit water yield along stemflow flow paths (Stubbins et al. 2020). Similarly, the deeply furrowed bark of sugar maple likely contributed to higher DOC concentrations than the smooth, papery bark of yellow birch. DOC and Ca^{2+} were most enriched in sugar maple stemflow (Fig. 2), possibly due to higher water absorption capacity of sugar maple bark and interactions of epiphytic fauna and biota along the stemflow flow path (McGee et al. 2019). Elevated DOC

Fig. 6 Selected solute concentrations and quantitative DOM optical metrics versus storm event size for **A, B, C** dissolved organic carbon (DOC), **D, E, F** Napierian absorbance coefficient at 254 nm (a_{254}), **G, H, I** the sum of PARAFAC component fluorescence (F_{tot}), and **J, K, L** dissolved calcium (Ca^{2+})



and Ca^{2+} concentrations and enrichment ratios indicate that trees substantially altered rainwater before it reached the forest floor, potentially providing important carbon sources for soil microbial communities and downstream ecosystems. Consideration of DOC and Ca^{2+} enrichment in throughfall and stemflow is of particular concern to studies estimating carbon budgets and weathering where data from open canopy weather stations do not accurately represent inputs to the forest floor.

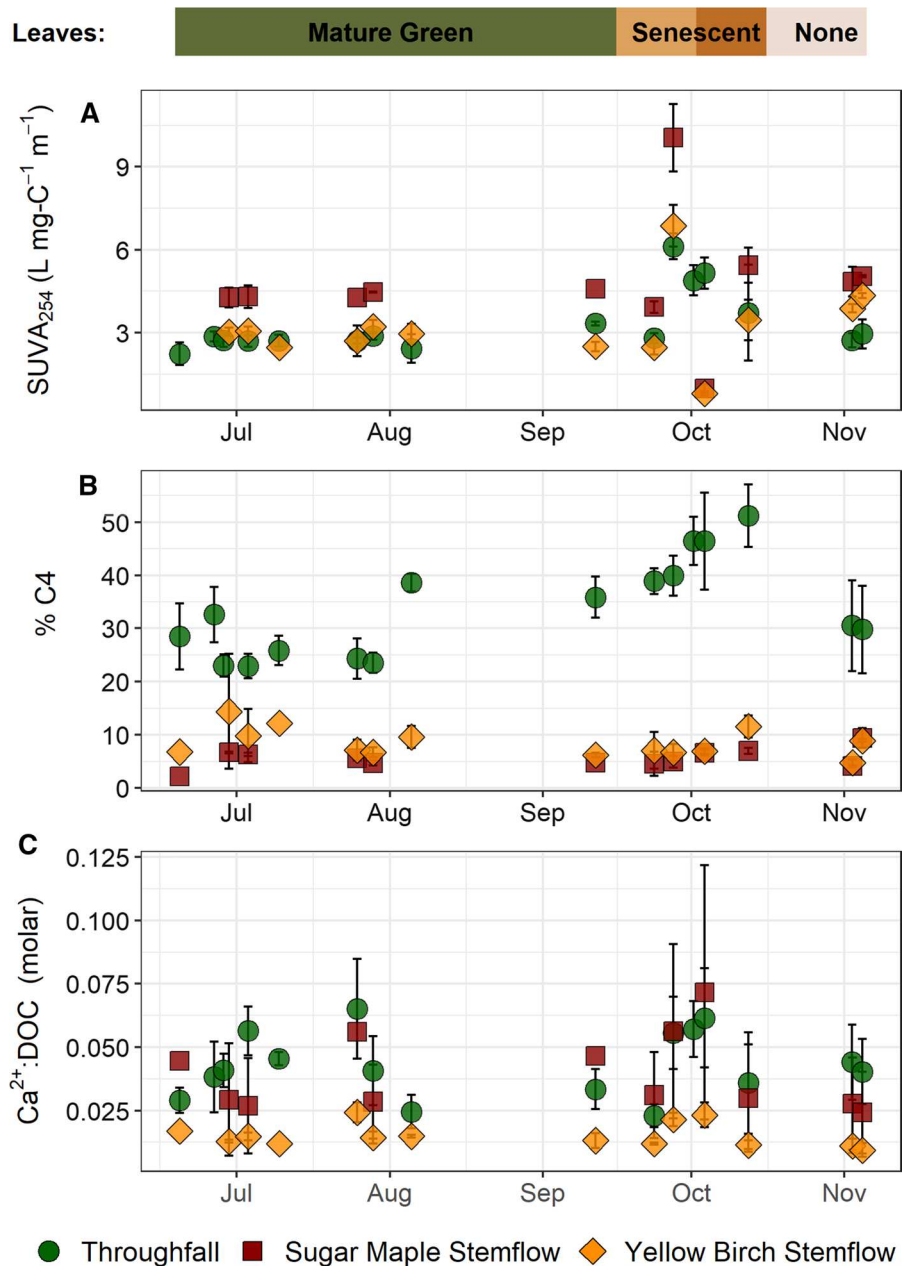
Dissolved organic matter optical properties

The a_{254} values observed here for rainfall (median $< 3 \text{ m}^{-1}$) are consistent with previous studies reporting low absorbance in rainwater ($< 4 \text{ m}^{-1}$ at 300 nm) (Yang et al. 2019). In comparison to precipitation, a_{254} values in throughfall (median $> 50 \text{ m}^{-1}$) and stemflow ($> 200 \text{ m}^{-1}$) were significantly elevated and confirm the general chromophoric nature of tree-derived DOM. Mean a_{254} for sugar maple

$(530 \pm 430 \text{ m}^{-1})$ and yellow birch $(230 \pm 150 \text{ m}^{-1})$ stemflow in this study were greater than the highest mean value reported for epiphyte-covered cedar trees in coastal Georgia $(60 \pm 30 \text{ m}^{-1}$; Van Stan et al. 2017), although values up to 526 m^{-1} were reported for southern live oak (Stubbins et al. 2017).

The observed approximate exponential decrease in absorbance with increasing wavelength was similar to previous absorbance spectra of throughfall and stemflow (Stubbins et al. 2017), leaf leachates (Frimmel and Bauer 1987; Zhao et al. 2020), and other natural waters (Massicotte et al. 2017). Spectral slopes for the log-linearized spectra between 275 and 295 nm ($S_{275-295}$) for throughfall and stemflow in this study (0.013 to 0.015 nm^{-1}) were similar to maple leaf litter leachates (0.012 to 0.015 nm^{-1} ; Meingast et al. 2020) and fell within the range for natural waters broadly (0.012 to 0.023 nm^{-1} ; Spencer et al. 2012). Previous reports of $S_{275-295}$ in rainwater are more variable (0.006 to 0.023 nm^{-1}) due to low chromophoric DOM concentrations (Yang et al. 2019). Decreasing $S_{275-295}$

Fig. 7 Throughfall and stemflow qualitative metrics
A SUVA₂₅₄, **B** percent PARAFAC component 4 (%C4), and **C** molar ratio of Ca²⁺ to DOC versus sample date



has been associated with increasing molecular weight in estuary waters (Helms et al. 2008). Although molecular weight was not measured in this study, Stubbins et al. (2017) used high resolution mass spectrometry to report higher molecular weight present in live oak stemflow ($S_{275-295}=0.014 \text{ nm}^{-1}$) compared to live oak throughfall ($S_{275-295}=0.016 \text{ nm}^{-1}$). If this relation broadly holds true for tree-derived DOM, our results suggest sugar maple stemflow (mean

$S_{275-295}=0.014 \text{ nm}^{-1}$) may be higher in molecular weight than yellow birch stemflow and throughfall (mean=0.015 nm⁻¹). Future studies investigating downstream processing of tree-derived DOM may reveal important ecological implications arising from differences in DOM composition due to species-specific sources.

The specific UV absorptance (SUVA₂₅₄) in throughfall and stemflow (range=2.9 to 4.5 L

$\text{mg-C}^{-1} \text{ m}^{-1}$) fell within the range reported for previous studies (1.7 to 6.3 $\text{L mg-C}^{-1} \text{ m}^{-1}$; Levia et al. 2012; Van Stan et al. 2017; Wagner et al. 2019), and United States rivers (1.3 to 4.6; Spencer et al. 2012). Higher SUVA₂₅₄ values indicate higher absorbance per unit carbon due generally to increased aromaticity of the DOM (Weishaar et al. 2003). The influence of iron was not considered a cause of high SUVA₂₅₄ values ($>5 \text{ L mg-C}^{-1} \text{ m}^{-1}$) because the ratio of iron to DOC in all samples was less than 0.1, an interference threshold previously determined by Poulin et al. (2014). SUVA₂₅₄ for sugar maple stemflow (median = 4.5 $\text{L mg-C}^{-1} \text{ m}^{-1}$) was higher than yellow birch and throughfall (medians = ~2.9 $\text{L mg-C}^{-1} \text{ m}^{-1}$), suggesting DOM in sugar maple stemflow contains more aromatic DOC compared to throughfall and yellow birch stemflow.

PARAFAC model results matched 87 previously reported components (>0.95 similarity score) in the OpenFluor database (Murphy et al. 2014). Humic-like components (C1, C2, and C3) matched fluorescence components described in headwater streams (Garcia et al. 2015; Graeber et al. 2012; Yamashita et al. 2011) and rivers of varied latitude and surrounding land use (Dalmagro et al. 2019; Lambert et al. 2016; Walker et al. 2013; Williams et al. 2010). Humic-like component C2 also matched fluorescence components published from peatland rivers (Zhou et al. 2019), plant material (Derrien et al. 2018), and forest soils more closely associated with plant-derived organics and fulvic acids (McKnight et al. 2001; Wu et al. 2021). Carboxylated lignin-derived aromatics are enriched in throughfall and stemflow (Guggenberger and Zech 1994) likely contributing to the humic-like DOM optical properties observed here. The protein-like component C4 matched fluorescence present in tropical rainforest throughfall (Osburn et al. 2018) and fresh DOM released from stream hyporheic zones (Harjung et al. 2018). In leaf leachates and other natural waters, fluorescence in the EEM region described as “protein-like” in this study has been shown to correlate with lower molecular weight molecules (Cuss and Gueguen 2013; Stubbins et al. 2014) and nitrogen-containing aromatics such as amino acids (e.g. tryptophan; Yamashita and Tanoue 2003). However, different compound classes containing different fluorophores can exhibit similar fluorescence properties (Aiken 2014; Wünsch et al. 2015). It may be more plausible that the fluorescence

of dissolved wash off and leachate from live vegetation in this study is derived from simple phenols, tannins, and lignin-derived polyphenols associated with plant materials. Further compound specific analyses would help elucidate the chemical composition of tree-derived fluorescent DOM.

Fluorescence signatures unique to throughfall and stemflow are difficult to discern since both humic-like and protein-like fluorescence co-occur in precipitation (Yang et al. 2019), throughfall and stemflow (Inamdar et al. 2012; Van Stan et al. 2017), and in leaf litter leachates (Cuss and Gueguen 2013; Wheeler et al. 2017). Throughfall and stemflow could be enriched in protein-like fluorescence from freshly leached or microbially produced DOM while also containing degraded DOM contributing to humic-like fluorescence. In this study, the lower overall fluorescence intensity (Fig. 4) and higher percentage of C4 (Fig. 5) in throughfall compared to stemflow is consistent with lower flow path residence times associated with throughfall supplying simpler and less diverse molecules. The higher variability of percent fluorescence components in precipitation is attributed to lower quantities of fluorescent DOM contributing to greater noise in the PARAFAC model for those samples. We found no relation between storm volume and percent PARAFAC components in precipitation. However, other studies have shown that rainwater originating from terrestrial air masses have higher DOC and humic-like fluorescence than marine sourced air masses (Yang et al. 2019). While protein-like fluorescence was also present in stemflow, the greater contact time of stemflow with tree surfaces could have allowed for a longer processing time of plant-derived DOM, degrading it into more diverse, complex aromatics contributing to a more dominant humic-like fluorescence signature.

In summary, tree-derived DOM is optically characterized by having higher a_{254} , lower $S_{275-295}$, higher SUVA₂₅₄, and a greater percentage of humic-like and protein-like fluorescence than DOM in rainfall. Classical interpretation of these DOM optical metrics suggests tree-derived DOM is comprised of a complex mixture of aromatic compounds including lower molecular weight simple phenols and higher molecular weight lignin-derived polyphenols. It is important to note that inferences about the chemical significance of DOM optical properties are based primarily upon work in rivers, lakes,

and the ocean. Further study is warranted to determine whether these classical interpretations of DOM optical properties hold for the presumably freshly produced DOM being washed from live vegetation. Regardless of the chemical composition of tree-derived DOM, differences in optical properties in this study indicate DOM quality varies between sugar maple and yellow birch trees. Thus, tree-derived DOM chemical composition is expected to vary across other tree species. Our results showing the prominence of longer wavelength emission (C2) in sugar maple stemflow (Figs. 4, 5) supports previous work demonstrating species-specific differences in DOM optical properties (Levia et al. 2012; Wheeler et al. 2017). In this system, the percentage of humic-like fluorescence (C2) distinguished between sugar maple and yellow birch stemflow, while the percentage of protein-like fluorescence (C4) was distinct for throughfall (Fig. 5B, Table S3). The ratios of these fluorescence regions are often calculated in common fluorescence indices (e.g.; fluorescence index). However, no index differentiated between sample flow paths as well as the percentages of PARAFAC components. Developed for aquatic systems, the fluorescence index (FI) is negatively correlated with aromaticity where values of ~ 1.4 are indicative of terrestrial derived DOM (McKnight et al. 2001). Mean FI determined for throughfall (1.5) and stemflow (1.4) in this study are consistent with terrestrial, aromatic, tree-derived sources. In leaf litter leachates, FI values can vary widely (1.3 to 2.0) but averaged 1.6 for naturally abscised cottonwood leaf leachates (Wymore et al. 2015). The biological index (BIX) was originally proposed to indicate autochthonous DOM sources in estuaries for values greater than one (Huguet et al. 2009). The low BIX reported for throughfall and stemflow in this study (~ 0.4) was also indicative of DOM associated with allochthonous sources in aquatic systems and was similar to mean values reported from sugar maple and paper birch leaf leachates (0.5) (Meingast et al. 2020). Future work should include PARAFAC analysis for improved precision when considering DOM optical properties as a DOM tracer through soils and downstream ecosystems. The overall variability of DOM optical metrics within throughfall and stemflow suggests additional hydrometeorological factors other than flow path and species influence DOM quality.

Climatic and seasonal effects

A general pattern of decreasing solute concentrations in throughfall and stemflow with increasing rain event volume has been described for both DOC (Comiskey 1978; Duval 2019; Ryan et al. 2021a; Van Stan et al. 2017) and inorganic ions (Germer et al. 2007; Levia et al. 2011). However, increases in solute concentrations with increasing event volume have also been reported potentially driven by variable precipitation intensity or the presence of dense epiphyte communities (Hansen et al. 1994; Van Stan et al. 2017). We interpret the decrease in DOC and Ca^{2+} concentrations with increasing event size, often described well by an exponential decay model (Fig. 6), as a result of dilution by rain of sources available to be washed off or leached from tree surfaces (Kazda 1990). Exponential decay slopes modeled in this study for DOC concentrations versus event size (0.07 to 0.24 mm^{-1}) were similar to those for a deciduous swamp (~ 0.03 mm^{-1}) in Ontario, Canada (Duval 2019) and for cedar and live oaks (~ 0.1 mm^{-1}) in the southeast United States (Van Stan et al. 2017). However, modeled slopes should be compared with caution since the range of storm event sizes available for each system and flow path as well as other statistical treatments of data prior to modeling can influence slope values. Similar to DOC, CDOM absorbance (a_{254}) and total fluorescence intensity (F_{tot}) showed dilution with increasing event volume precluding the examination of phenoseasonal trends for these variables in this study.

Decreasing DOM concentrations in throughfall and stemflow for larger events suggest that the first pulse of DOM-rich water occurring early within an event may define the bulk DOM composition of throughfall and stemflow for a given event. Qualitative DOM optical metrics (e.g., $S_{275:295}$, SUVA_{254} , % PARAFAC components) did not show dilution trends using linear or log-linear models (Table S4; $p > 0.3$) indicating that flow path type was the principal factor controlling DOM optical properties while event size exerted minor influence. Thus, the minimal influence of event size on DOM quality allowed comparison of DOM optical properties across phenoseasons (Fig. 7). During the fall season, the leaching of organic pigments from leaves during senescence likely influenced the increase in SUVA_{254} in throughfall due to anthocyanin and carotenoid pigments which are

responsible for fall colors (Lee et al. 2003). The variability of SUVA₂₅₄ also increased during fall storms, particularly for stemflow (Fig. 7A). SUVA₂₅₄ values considered high ($> 5 \text{ L mg-C}^{-1} \text{ m}^{-1}$) and low ($< 1 \text{ L mg-C}^{-1} \text{ m}^{-1}$) did not correspond with unusually large or small rain events and have been previously reported for rain and throughfall (Levia et al. 2012; Stubbins et al. 2017). Changes in SUVA₂₅₄ could be caused by processes that remove aliphatic molecules (e.g., microbial respiration) or add aromatics (e.g., vegetation leachates). River water contains a blended mixture of both aliphatic and aromatic DOM from multiple sources and thus typically ranges from 1.3 to 4.6 L mg-C⁻¹ m⁻¹ (Spencer et al. 2012). However, Weishaar et al. (2003) estimated that a SUVA₂₅₄ of 6 corresponds to approximately 50% aromaticity which suggests some stemflow samples in this study could have reached nearly 80% aromaticity. Overall, the increased variability of SUVA₂₅₄ underscores the importance of measuring individual storm events where DOM dynamics may not be detected in monthly or seasonally integrated samples.

While Ca²⁺ and DOC concentrations could not be compared across seasons due to the influence of event volume on these solute concentrations, Ca^{2+**:DOC} was elevated in fall versus summer storms indicating leaching and wash off processes associated with these solutes may differ across seasons. Organic matter content and leachable ions such as Ca²⁺ have previously been shown to increase in throughfall during senescence due to physiological changes or physical deterioration of leaf cuticles (Eaton et al. 1973). Hudson et al. (2018) reported an increase in SUVA₂₅₄ in water extractions of senescent versus non-senescent American beech leaves across the eastern United States. Consistent with these studies, our data show an increase in percent protein-like fluorescence (%C4) in throughfall during the senescent period (Fig. 7) suggesting that increased leaching of aromatic pigments associated with senescent leaves are driving this pattern. Wheeler et al. (2017) reported an overall increase in the proportion of humic-like fluorescence in leaf extracts during senescence in four sites in the eastern United States. However, two of the three protein-like fluorescence components in the Wheeler et al. (2017) study also increased along an increasing senescence gradient. Comparisons between throughfall and leaf leachate study results are complicated by the rinsing and cutting of leaf litter prior

to leaching experiments which removes material that is most likely washed from leaf surfaces by throughfall. Microbial-derived DOM is one additional possible contributing source to protein-like fluorescence in throughfall and future studies quantifying microbial activity on leaf surfaces during senescence may help elucidate this contribution. In this study, changes in stemflow DOM quality were not consistently different between mature leaf and senescent leaf types possibly due to the limited interactions of stemflow with changing leaves while bark characteristics remain more similar across seasons.

Increasing temperature, growing season length, precipitation, and storm intensity in the New England region of the United States due to climate change is likely to change the timing of tree-derived DOM fluxes delivered to the forest floor (Huntington et al. 2009; Ryan et al. 2021a). Similarly, changing phenoseason timing also impacts tree-derived solutes and DOM quality (Wheeler et al. 2017). Solute leaching from leaves is typically least during leaf emergence and greatest during senescence (Van Stan et al. 2012). Winters have greater relative warming due to climate change (Campbell et al. 2005). Thus, more tree-derived DOM is likely to be delivered to soils earlier in the growing season while fall senescence is likely to be delayed under future warming (Estiarte and Penuelas 2015). Over longer time scales shifting distribution of tree species could influence species-specific tree-derived DOM quality (Iverson and Prasad 2002). Given the importance of annual leaf litter processing in aquatic ecosystems (McDowell and Fisher 1976) and the potential of tree-derived DOM to contribute to harmful disinfection byproducts during drinking water treatment (Chen et al. 2019; Chow et al. 2009), understanding the factors controlling tree-derived DOM quality is an important scientific goal. In this study, phenoseason did not impact the amount of DOM delivered to the forest floor (Fig. 6). However, phenoseason did impact the quality of DOM in throughfall. Thus, future studies should consider phenoseason as an important factor influencing throughfall and stemflow DOM quality.

Conclusion

Precipitation partitioning by the mixed hardwood forest in Sleepers River Research Watershed enriched

throughfall and stemflow in DOM and Ca^{2+} relative to rainwater. Stemflow from sugar maple and yellow birch trees was more enriched than throughfall, and sugar maple stemflow was more enriched than yellow birch stemflow, likely due to differing flow path water residence times and bark characteristics. Further work is needed to incorporate the substantial enrichment of throughfall and stemflow in modeling the response of soil and downstream ecosystems to precipitation.

DOM optical metrics in throughfall and stemflow in this study were characteristic of complex mixtures of aromatic compounds similar to those reported previously for tree-derived DOM broadly (Van Stan and Stubbins 2018). The PARAFAC model of DOM fluorescence distinguished DOM in throughfall, stemflow, and rainfall according to percent protein-like (%C4) versus percent humic-like (%C2) fluorescence more effectively than traditional EEM indices. Thus, future studies could assess whether the considerable differences in DOM optical properties between throughfall and stemflow could be used to inform DOM loss mechanisms along subsurface flow paths to streams.

The apparent dilution of DOM and Ca^{2+} washed and leached from tree surfaces with increasing storm volume did not impact DOM optical properties. However, DOM optical properties were altered by phenoseason. These results support our initial hypothesis and suggest that flow paths and species composition are fundamental factors influencing DOM optical properties. As growing seasons for temperate forests increase in duration, we expect increased annual fluxes of DOM in throughfall and stemflow associated with mature leaves phenotype that appear earlier in the growing season. Thus models of DOM transport through forested ecosystems should be used to probe the implications of differing DOM quality in throughfall and stemflow across species and phenoseason. Future studies that advance understanding of tree-derived DOM quality will allow more robust accounting of carbon transfers across terrestrial-aquatic boundaries.

Acknowledgements The authors thank Miles Despathy and Russell Desclos for assistance with field measurements and the Forestry Sciences Laboratory in Grand Rapids, Minnesota for cation analyses. The authors are grateful to John Larson (USFS) and Keith Oleheiser (Oak Ridge National Laboratory) for their contributions to lab analyses. We thank Mackenzie Fiss (Northeastern University) and two anonymous reviewers for their helpful comments.

Author contribution Conceptualization: KAR, AC, JP, JBS, AS. Methodology: KAR, TA, AC, JP, JBS, SS, AS. Writing—original draft preparation: KAR. Writing—review and editing: KAR, JP, JBS, SS, AS.

Funding JBS was supported by United States Geological Survey Climate R&D. KAR was supported by a United States National Science Foundation Graduate Student Preparedness Fellowship. JP was supported by United States National Science Foundation Grants EAR 2012123 and EAR 1724171. TA was supported by NSF EAR 1724171. The USDA Forest Service Northern Research Station funded the contributions of SDS to this work.

Data availability Data are available in the published USGS ScienceBase data release (Ryan et al. 2021b).

Declarations

Conflict of interest The authors have no relevant financial or non-financial interests to disclose. Any use of trade, firm, or product names is for descriptive purposes only and does not imply endorsement by the U.S. Government.

Open Access This article is licensed under a Creative Commons Attribution 4.0 International License, which permits use, sharing, adaptation, distribution and reproduction in any medium or format, as long as you give appropriate credit to the original author(s) and the source, provide a link to the Creative Commons licence, and indicate if changes were made. The images or other third party material in this article are included in the article's Creative Commons licence, unless indicated otherwise in a credit line to the material. If material is not included in the article's Creative Commons licence and your intended use is not permitted by statutory regulation or exceeds the permitted use, you will need to obtain permission directly from the copyright holder. To view a copy of this licence, visit <http://creativecommons.org/licenses/by/4.0/>.

References

- Aiken G (2014) Fluorescence and dissolved organic matter: a chemist's perspective. In: Baker A, Reynolds DM, Lead J, Coble PG, Spencer RGM (eds) Aquatic organic matter fluorescence. Cambridge environmental chemistry series. Cambridge University Press, Cambridge, pp 35–74
- Angelini IM, Garstang M, Davis RE, Hayden B, Fitzjarrald DR, Legates DR, Greco S, Macko S, Connors V (2011) On the coupling between vegetation and the atmosphere. *Theoret Appl Climatol* 105(1–2):243–261

Behnke MI, Fellman JB, D'Amore DV, Gomez SM, Spencer RGM (2022) From canopy to consumer: what makes and modifies terrestrial DOM in a temperate forest. *Biogeochemistry*:

Bro R (1997) PARAFAC. Tutorial and applications. *Chemometr Intell Lab Syst* 38(2):149–171

Campbell JL, Mitchell MJ, Groffman PM, Christenson LM, Hardy JP (2005) Winter in northeastern North America: a critical period for ecological processes. *Front Ecol Environ* 3(6):314–322

Chen H, Tsai K-P, Su Q, Chow AT, Wang J-J (2019) Through-fall dissolved organic matter as a terrestrial disinfection byproduct precursor. *ACS Earth Space Chem* 3(8):1603–1613

Chow AT, Lee ST, O'Geen AT, Orozco T, Beaudette D, Wong PK, Hernes PJ, Tate KW, Dahlgren RA (2009) Litter contributions to dissolved organic matter and disinfection byproduct precursors in California oak woodland watersheds. *J Environ Qual* 38(6):2334–2343

Coble PG (1996) Characterization of marine and terrestrial DOM in seawater using excitation-emission matrix spectroscopy. *Mar Chem* 51(4):325–346

Comiskey CE (1978) Aspects of the organic carbon cycle on Walker Branch Watershed: a study in land/water interaction. In: University of Tennessee, p 509

Cuss CW, Gueguen C (2013) Distinguishing dissolved organic matter at its origin: size and optical properties of leaf-litter leachates. *Chemosphere* 92(11):1483–1489

Cuss CW, Guégan C (2015) Characterizing the labile fraction of dissolved organic matter in leaf leachates: methods, indicators, structure, and complexity. In: Labile organic matter-chemical compositions, function, and significance in soil and the environment. SSSA Special Publications, pp 237–274

Dalmagro H, Lathuillière M, Sallo F, Guerreiro M, Pinto O, de Arruda P, Couto E, Johnson M (2019) Streams with riparian forest buffers versus impoundments differ in discharge and DOM characteristics for pasture catchments in Southern Amazonia. *Water* 11(2):390

DeKett RG, Long RF (1995) Order 1 soil mapping project of the W-9 Basin in the Sleepers River watershed. In: United States Department of Agriculture Natural Resources Conservation Service, p 66

Derrien M, Kim MS, Ock G, Hong S, Cho J, Shin KH, Hur J (2018) Estimation of different source contributions to sediment organic matter in an agricultural-forested watershed using end member mixing analyses based on stable isotope ratios and fluorescence spectroscopy. *Sci Total Environ* 618:569–578

Drake TW, Raymond PA, Spencer RGM (2018) Terrestrial carbon inputs to inland waters: a current synthesis of estimates and uncertainty. *Limnol Oceanogr Lett* 3(3):132–142

Duval TP (2019) Rainfall partitioning through a mixed cedar swamp and associated C and N fluxes in Southern Ontario. *Canada Hydrol Process* 33(11):1510–1524

Eaton JS, Likens GE, Bormann FH (1973) Throughfall and stemflow chemistry in a Northern Hardwood Forest. *J Ecol* 61(2):495–508

Estiarte M, Penuelas J (2015) Alteration of the phenology of leaf senescence and fall in winter deciduous species by climate change: effects on nutrient proficiency. *Glob Chang Biol* 21(3):1005–1017

Fellman JB, Hood E, Spencer RGM (2010) Fluorescence spectroscopy opens new windows into dissolved organic matter dynamics in freshwater ecosystems: a review. *Limnol Oceanogr* 55(6):2452–2462

Frimmel FH, Bauer H (1987) Influence of photochemical reactions on the optical properties of aquatic humic substances gained from fall leaves. *Sci Total Environ* 62:139–148

Garcia RD, Reissig M, Queimaliños CP, Garcia PE, Dieguez MC (2015) Climate-driven terrestrial inputs in ultraoligotrophic mountain streams of Andean Patagonia revealed through chromophoric and fluorescent dissolved organic matter. *Sci Total Environ* 521–522:280–292

Germer S, Neill C, Krusche AV, Neto SCG, Elsenbeer H (2007) Seasonal and within-event dynamics of rainfall and throughfall chemistry in an open tropical rainforest in Rondônia, Brazil. *Biogeochemistry* 86(2):155–174

Graeber D, Gelbrecht J, Pusch MT, Anlanger C, von Schiller D (2012) Agriculture has changed the amount and composition of dissolved organic matter in Central European headwater streams. *Sci Total Environ* 438:435–446

Guggenberger G, Zech W (1994) Composition and dynamics of dissolved carbohydrates and lignin-degradation products in two coniferous forests, N.E. Bavaria, Germany. *Soil Biol Biochem* 26(1):19–27

Hansen AM, Fleck JA, Kraus TEC, Downing BD, von Dessen-neck T, Bergamaschi BA (2018) Procedures for using the Horiba Scientific Aqualog® fluorometer to measure absorbance and fluorescence from dissolved organic matter: U.S. Geological Survey Open-File Report 2018–1096. <https://doi.org/10.3133/ofr20181096>

Hansen AM, Kraus TEC, Pellerin BA, Fleck JA, Downing BD, Bergamaschi BA (2016) Optical properties of dissolved organic matter (DOM): effects of biological and photolytic degradation. *Limnol Oceanogr* 61(3):1015–1032

Hansen K, Draaijers G, Ivens W, Gundersen P, Vanleeuwen N (1994) Concentration variations in rain and canopy throughfall collected sequentially during individual rain events. *Atmos Environ* 28(20):3195–3205

Harjung A, Sabater F, Butturini A (2018) Hydrological connectivity drives dissolved organic matter processing in an intermittent stream. *Limnologica* 68:71–81

Helms JR, Stubbins A, Ritchie JD, Minor EC, Kieber DJ, Mopper K (2008) Absorption spectral slopes and slope ratios as indicators of molecular weight, source, and photobleaching of chromophoric dissolved organic matter. *Limnol Oceanogr* 53(3):955–969

Henderson GS, Harris WF, Todd DE, Grizzard T (1977) Quantity and chemistry of throughfall as influenced by forest-type and season. *J Ecol* 65(2):365–374

Hernes PJ, Spencer RGM, Dyda RY, O'Geen AT, Dahlgren RA (2017) The genesis and exodus of vascular plant DOM from an Oak Woodland Landscape. *Front Earth Sci* 5:9

Hewlett JD (1982) Principles of forest hydrology. University of Georgia Press, Athens, GA

Howard D, Stan J, Whitetree A, Zhu L, Stubbins A (2018) Interstorm variability in the biolability of tree-derived dissolved organic matter (tree-DOM) in throughfall and stemflow. *Forests* 9(5):236

Hudson JE, Levia DF, Wheeler KI, Winters CG, Vaughan MCH, Chace JF, Sleeper R (2018) American beech leaf-litter leachate chemistry: effects of geography and phenophase. *J Plant Nutr Soil Sci* 181(2):287–295

Huguet A, Vacher L, Relexans S, Saubusse S, Froidefond JM, Parlanti E (2009) Properties of fluorescent dissolved organic matter in the Gironde Estuary. *Org Geochem* 40(6):706–719

Huntington TG, Richardson AD, McGuire KJ, Hayhoe K (2009) Climate and hydrological changes in the Northeastern United States: recent trends and implications for forested and aquatic ecosystems. *Can J for Res* 39(2):199–212

Hutjes RWA, Kabat P, Running SW, Shuttleworth WJ, Field C, Bass B, da Silva Dias MF, Avissar R, Becker A, Claussen M, Dolman AJ, Feddes RA, Fosberg M, Fukushima Y, Gash JHC, Guenni L, Hoff H, Jarvis PG, Kayane I, Krenke AN, Liu C, Meybeck M, Nobre CA, Oyebande L, Pitman A, Pielke RA Sr, Raupach M, Saugier B, Schulze ED, Sellers PJ, Tenhunen JD, Valentini R, Victoria RL, Vörösmarty CJ (1998) Biospheric aspects of the hydrological cycle. *J Hydrol* 212–213:1–21

Iavorivska L, Boyer EW, DeWalle DR (2016) Atmospheric deposition of organic carbon via precipitation. *Atmos Environ* 146:153–163

Inamdar S, Finger N, Singh S, Mitchell M, Levia D, Bais H, Scott D, McHale P (2012) Dissolved organic matter (DOM) concentration and quality in a forested mid-Atlantic watershed, USA. *Biogeochemistry* 108(1):55–76

Inamdar S, Singh S, Dutta S, Levia D, Mitchell M, Scott D, Bais H, McHale P (2011) Fluorescence characteristics and sources of dissolved organic matter for stream water during storm events in a forested mid-Atlantic watershed. *Journal of Geophysical Research: Biogeosciences* 116(G3):

Iverson LR, Prasad AM (2002) Potential redistribution of tree species habitat under five climate change scenarios in the eastern US. *For Ecol Manage* 155(1–3):205–222

Kazda M (1990) Sequential stemflow sampling for estimation of dry deposition and crown leaching in beech stands. Elsevier Applied Science Publishers Ltd., Barking, pp 46–55

Kirk JTO (1994) Absorption of light within the aquatic medium. In: Kirk JTO (ed) *Light and photosynthesis in aquatic ecosystems*. Cambridge University Press, Cambridge, pp 46–84

Lambert T, Bouillon S, Darchambeau F, Massicotte P, Borges AV (2016) Shift in the chemical composition of dissolved organic matter in the Congo River network. *Biogeosciences* 13(18):5405–5420

Lawaetz AJ, Stedmon CA (2009) Fluorescence intensity calibration using the Raman scatter peak of water. *Appl Spectrosc* 63(8):936–940

Lee DW, O'Keefe J, Holbrook NM, Feild TS (2003) Pigment dynamics and autumn leaf senescence in a New England deciduous forest, eastern USA. *Ecol Res* 18(6):677–694

Leonard RE (1961) Interception of precipitation by northern hardwoods. In: U.S. Department of Agriculture FS, Northeastern Forest Experiment Station (ed). *Upper Darby, PA*, p 16

Levia DF, Frost EE (2006) Variability of throughfall volume and solute inputs in wooded ecosystems. *Progress Phys Geogr Earth Environ* 30(5):605–632

Levia DF, Germer S (2015) A review of stemflow generation dynamics and stemflow-environment interactions in forests and shrublands. *Rev Geophys* 53(3):673–714

Levia DF, Herwitz SR (2005) Interspecific variation of bark water storage capacity of three deciduous tree species in relation to stemflow yield and solute flux to forest soils. *CATENA* 64(1):117–137

Levia DF, Van Stan JT, Inamdar SP, Jarvis MT, Mitchell MJ, Mage SM, Scheick CE, McHale PJ (2012) Stemflow and dissolved organic carbon cycling: temporal variability in concentration, flux, and UV-Vis spectral metrics in a temperate broadleaved deciduous forest in the eastern United States. *Can J for Res* 42(1):207–216

Levia DF, Van Stan JT, Mage SM, Kelley-Hauske PW (2010) Temporal variability of stemflow volume in a beech-yellow poplar forest in relation to tree species and size. *J Hydrol* 380(1–2):112–120

Levia DF, Van Stan JT, Siegert CM, Inamdar SP, Mitchell MJ, Mage SM, McHale PJ (2011) Atmospheric deposition and corresponding variability of stemflow chemistry across temporal scales in a mid-Atlantic broadleaved deciduous forest. *Atmos Environ* 45(18):3046–3054

Massicotte P, Asmala E, Stedmon C, Markager S (2017) Global distribution of dissolved organic matter along the aquatic continuum: across rivers, lakes and oceans. *Sci Total Environ* 609:180–191

McClain ME, Boyer EW, Dent CL, Gergel SE, Grimm NB, Groffman PM, Hart SC, Harvey JW, Johnston CA, Mayorga E, McDowell WH, Pinay G (2003) Biogeochemical hot spots and hot moments at the interface of terrestrial and aquatic ecosystems. *Ecosystems* 6(4):301–312

McDowell WH, Fisher SG (1976) Autumnal processing of dissolved organic matter in a small woodland stream ecosystem. *Ecology* 57(3):561–569

McDowell WH, Likens GE (1988) Origin, composition, and flux of dissolved organic carbon in the Hubbard Brook valley. *Ecol Monogr* 58(3):177–195

McGee GG, Cardon ME, Kiernan DH (2019) Variation in acer saccharum marshall (sugar maple) bark and stemflow characteristics: implications for epiphytic bryophyte communities. *Northeastern Nat* 26(1):214–235

McKnight DM, Boyer EW, Westerhoff PK, Doran PT, Kulbe T, Andersen DT (2001) Spectrofluorometric characterization of dissolved organic matter for indication of precursor organic material and aromaticity. *Limnol Oceanogr* 46(1):38–48

Meingast KM, Grunert BK, Green SA, Kane ES, Khademimoshgenani N (2020) Insights on dissolved organic matter production revealed by removal of charge-transfer interactions in senescent leaf leachates. *Water* 12(9):2356

Mulholland PJ (2002) Large-scale patterns in dissolved organic carbon concentration, flux, and sources. In: Findlay S, Sinsabaugh RL (eds) *Aquatic ecosystems: interactivity of dissolved organic matter*. Elsevier Science & Technology, Burlington, pp 139–160

Murphy KR, Stedmon CA, Graeber D, Bro R (2013) Fluorescence spectroscopy and multi-way techniques. *PARAFAC. Anal Methods* 5(23):6557–6566

Murphy KR, Stedmon CA, Wenig P, Bro R (2014) Open-Fluor— an online spectral library of auto-fluorescence by organic compounds in the environment. *Anal Methods* 6(3):658–661

Ohno T (2002) Fluorescence inner-filtering correction for determining the humification index of dissolved organic matter. *Environ Sci Technol* 36(4):742–746

Osburn CL, Oviedo-Vargas D, Barnett E, Dierick D, Oberbauer SF, Genereux DP (2018) Regional groundwater and storms are hydrologic controls on the quality and export of dissolved organic matter in two tropical rainforest streams, Costa Rica. *J Geophys Res Biogeosci* 123(3):850–866

Park BB, Yanai RD, Fahey TJ, Bailey SW, Siccama TG, Shanley JB, Cleavitt NL (2008) Fine root dynamics and forest production across a calcium gradient in northern hardwood and conifer ecosystems. *Ecosystems* 11(2):325–341

Ponette-González AG, Ewing HA, Weathers KC, Johnson EA, Martin YE (2016) Interactions between precipitation and vegetation canopies. In: A biogeoscience approach to ecosystems, pp 215–253

Ponette-González AG, Van Stan JT, Magyar D (2020) Things seen and unseen in throughfall and stemflow. In: Precipitation partitioning by vegetation, pp 71–88

Poulin BA, Ryan JN, Aiken GR (2014) Effects of iron on optical properties of dissolved organic matter. *Environ Sci Technol* 48(17):10098–10106

Pucher M, Wünsch U, Weigelhofer G, Murphy K, Hein T, Graeber D (2019) staRdom: versatile software for analyzing spectroscopic data of dissolved organic matter in R. *Water* 11(11):2366

Qualls RG (2020) Role of precipitation partitioning in litter biogeochemistry. In: Precipitation partitioning by vegetation, pp 163–182

Qualls RG, Haines BL (1992) Biodegradability of dissolved organic matter in forest throughfall, soil solution, and stream water. *Soil Sci Soc Am J* 56(2):578–586

Ryan KA, Adler T, Chalmers A, Perdrial J, Shanley JB, Stubbins A (2021a) Event scale relationships of DOC and TDN fluxes in throughfall and stemflow diverge from stream exports in a forested catchment. *J Geophys Res Biogeo.* <https://doi.org/10.1029/2021JG006281>

Ryan KA, Shanley JB, Adler T, Chalmers A, Perdrial J, Stubbins A (2021b) Storm event dissolved organic carbon and total dissolved nitrogen concentrations and yields for precipitation, throughfall, stemflow and stream water and hourly streamflow and precipitation record for the W-9 catchment, Sleepers River Research Watershed, 2017 and 2018 (ver. 2.0): U.S. Geological Survey data release. <https://doi.org/10.5066/P9OCS8P7>

Sadeghi SMM, Gordon DA, Van Stan II JT (2020) A Global Synthesis of Throughfall and Stemflow Hydrometeorology. In: Van Stan II JT, Gutmann E & Friesen J (eds) *Precipitation Partitioning by Vegetation: A Global Synthesis*. Springer International Publishing, Cham. pp 49–70

Sebestyen SD, Oleheiser KC, Larson JT, N.A. Aspelin, Stelling JM, Griffiths NA, Lany NK (2020) Marcell experimental forest event based precipitation chemistry, 2008 – ongoing ver 1. *Environmental Data Initiative*

Shanley JB (2000) Sleepers river, vermont: a water, energy, and biogeochemical budgets program site. United States Geological Survey. Fact Sheet, pp 166–99

Shanley JB, Chalmers AT, Denner JC, Clark SF (2021) Five-minute discharge; daily precipitation, stream runoff, and maximum and minimum air temperature; and annual precipitation and runoff for W-9 catchment, Sleepers River Research Watershed near Danville, Vermont, 1991–2018: U.S. Geological Survey data release

Shanley JB, Krám P, Hruška J, Bullen TD (2004) A Biogeochemical Comparison of Two Well-Buffered Catchments with Contrasting Histories of Acid Deposition. *Water Air Soil Pollut Focus* 4(2/3):325–342

Shanley JB, Sebestyen SD, McDonnell JJ, McGlynn BL, Dunne T (2015) Water's Way at Sleepers River watershed: revisiting flow generation in a post-glacial landscape, Vermont USA. *Hydrol Process* 29(16):3447–3459

Siegert CM, Levia DF, Leathers DJ, Van Stan JT, Mitchell MJ (2017) Do storm synoptic patterns affect biogeochemical fluxes from temperate deciduous forest canopies? *Biogeochemistry* 132(3):273–292

Singh S, Inamdar S, Mitchell M (2015) Changes in dissolved organic matter (DOM) amount and composition along nested headwater stream locations during baseflow and stormflow. *Hydrol Process* 29(6):1505–1520

Spencer RGM, Butler KD, Aiken GR (2012) Dissolved organic carbon and chromophoric dissolved organic matter properties of rivers in the USA. *J Geophys Res* 117(G3): n/a-n/a

Stubbins A, Guillemette F, Van Stan II JT (2020) Throughfall and stemflow: the crowning headwaters of the aquatic carbon cycle. In: Precipitation partitioning by vegetation, pp 121–132

Stubbins A, Lapierre JF, Berggren M, Prairie YT, Dittmar T, del Giorgio PA (2014) What's in an EEM? Molecular signatures associated with dissolved organic fluorescence in boreal Canada. *Environ Sci Technol* 48(18):10598–10606

Stubbins A, Silva LM, Dittmar T, Van Stan JT (2017) Molecular and optical properties of tree-derived dissolved organic matter in throughfall and stemflow from live oaks and eastern red cedar. *Front Earth Sci.* <https://doi.org/10.3389/feart.2017.00022>

Tanase C, Cosarca S, Muntean DL (2019) A critical review of phenolic compounds extracted from the bark of woody vascular plants and their potential biological activity. *Molecules* 24(6):1182

Van Stan JT, Levia DF, Inamdar SP, Lepori-Bui M, Mitchell MJ (2012) The effects of phenoseason and storm characteristics on throughfall solute washoff and leaching dynamics from a temperate deciduous forest canopy. *Sci Total Environ* 430:48–58

Van Stan JT, Stubbins A (2018) Tree-DOM: dissolved organic matter in throughfall and stemflow. *Limnol Oceanogr Lett* 3(3):199–214

Van Stan JT, Wagner S, Guillemette F, Whitetree A, Lewis J, Silva L, Stubbins A (2017) Temporal dynamics in the concentration, flux, and optical properties of tree-derived dissolved organic matter in an epiphyte-Laden Oak-Cedar Forest. *J Geophys Res Biogeosci* 122(11):2982–2997

Wagner S, Brantley S, Stuber S, Van Stan J, Whitetree A, Stubbins A (2019) Dissolved black carbon in throughfall and stemflow in a fire-managed longleaf pine woodland. *Biogeochemistry* 146:191–207

Walker SA, Amon RMW, Stedmon CA (2013) Variations in high-latitude riverine fluorescent dissolved organic matter: A comparison of large Arctic rivers. *J Geophys Res Biogeosci* 118(4):1689–1702

Weishaar JL, Aiken GR, Bergamaschi BA, Fram MS, Fujii R, Mopper K (2003) Evaluation of specific ultraviolet absorbance as an indicator of the chemical composition and reactivity of dissolved organic carbon. *Environ Sci Technol* 37(20):4702–4708

Wheeler KI, Levia DF, Hudson JE (2017) Tracking senescence-induced patterns in leaf litter leachate using parallel factor analysis (PARAFAC) modeling and self-organizing maps. *J Geophys Res Biogeosci* 122(9):2233–2250

Williams CJ, Yamashita Y, Wilson HF, Jaffé R, Xenopoulos MA (2010) Unraveling the role of land use and microbial activity in shaping dissolved organic matter characteristics in stream ecosystems. *Limnol Oceanogr* 55(3):1159–1171

Wu H, Xu X, Fu P, Cheng W, Fu C (2021) Responses of soil WEOM quantity and quality to freeze–thaw and litter manipulation with contrasting soil water content: a laboratory experiment. *CATENA* 198:105058

Wünsch UJ, Murphy KR, Stedmon CA (2015) Fluorescence quantum yields of natural organic matter and organic compounds: implications for the fluorescence-based interpretation of organic matter composition. *Front Mar Sci.* <https://doi.org/10.3389/fmars.2015.00098>

Wymore AS, Compson ZG, McDowell WH, Potter JD, Hungate BA, Whitham TG, Marks JC (2015) Leaf-litter leachate is distinct in optical properties and bio-availability to stream heterotrophs. *Freshwater Science* 34(3):857–866

Yamashita Y, Kloepel BD, Knoepp J, Zausen GL, Jaffé R (2011) Effects of watershed history on dissolved organic matter characteristics in headwater streams. *Ecosystems* 14(7):1110–1122

Yamashita Y, Tanoue E (2003) Chemical characterization of protein-like fluorophores in DOM in relation to aromatic amino acids. *Mar Chem* 82(3–4):255–271

Yang L, Chen W, Zhuang W-E, Cheng Q, Li W, Wang H, Guo W, Chen C-TA, Liu M (2019) Characterization and bio-availability of rainwater dissolved organic matter at the southeast coast of China using absorption spectroscopy and fluorescence EEM-PARAFAC. *Estuar Coast Shelf Sci* 217:45–55

Zhao L, Du C, Zhang Q, Sun C, Wang S, Luo S (2020) The ultraviolet-visible absorbance and fluorescence characterization of dissolved organic matter derived from the leaf litter of *Populus simonii*, *Artemisia desertorum*, *Salix cheilophila*, and *Populus tomentosa*. *Environ Sci Pollut Res Int* 27(29):36439–36449

Zhou Y, Martin P, Müller M (2019) Composition and cycling of dissolved organic matter from tropical peatlands of coastal Sarawak, Borneo, revealed by fluorescence spectroscopy and parallel factor analysis. *Biogeosciences* 16(13):2733–2749

Publisher's Note Springer Nature remains neutral with regard to jurisdictional claims in published maps and institutional affiliations.